$l_{1/2}$-SVD Based Channel Estimation for MmWave Massive MIMO

Xiaoli Jing, Xianpeng Wang, Xiang Lan, and Liangtian Wan

1 Introduction

mmWave massive MIMO technology has the advantages of ultra-high transmission rate, large transmission bandwidth and lower transmission delay, it has become one of the important development trends of next generation mobile communication [1]. However, mmWave massive MIMO still faces technical problems such as serious reflection loss, multipath delay, and easy blocking interruption. These problems have brought challenges to channel estimation [2].

In recent years, the channel estimation algorithms based on compressed sensing (CS) mainly include greedy algorithms and convex optimization algorithms. Orthogonal Matching Pursuit (OMP) is a representative algorithm in greedy algorithms [3, 4]. But the greedy estimation algorithm is more likely to fall into the local optimal solution. Another type of recovery algorithm is to construct the sparse recovery problem as a l_0-norm optimization problem. It is more difficult to find the optimal result. Therefore, the convex optimization estimation algorithm is usually used to approximate. [5] proposed a l_1-norm-based channel estimation scheme, which reconstructs the problem of CS. However, in practice, due to the influence of random noise, the sparsest solution cannot be obtained in the l_1-norm solution. Rong et al. [6] has clearly pointed out that $l_q (0 < q < 1)$-norm has obtained a more sparse solution, but the quantization of the angle may introduce errors, so the channel estimation algorithm needs further improvement. In [7], an objective function based on $l_{1/2}$-regularization was constructed, and then the super-resolution channel estimation

X. Jing · X. Wang (✉) · X. Lan
State Key Laboratory of Marine Resource Utilization in South China Sea and School of Information and Communication Engineering, Hainan University, Haikou 570228, China
e-mail: wxpeng1986@126.com

L. Wan
School of Software, Dalian University of Technology, Dalian 116024, China

L. C. Jain et al. (eds.), *Advances in Wireless Communications and Applications*, Smart Innovation, Systems and Technologies 299,
https://doi.org/10.1007/978-981-19-2255-8_2

was finally realized through iterative optimization. However, the method proposed in this document is still unable to achieve the desired effect in terms of complexity.

The paper proposes a novel mmWave massive MIMO channel estimation algorithm. First, an objective function based on $l_{1/2}$-regularization is constructed. Then, the channel estimation problem is transformed into an alternative optimization problem through the gradient descent method, and the optimal angle parameter estimation value is obtained.

2 System Model

Under the system of hybrid-precoding mmWave massive MIMO, the transmit antennas is equipped with N_{t} antennas, the receiving end is equipped with N_{r} antennas. The number of transmitter RF chains and receiver RF chains are N_{t}^{RF} and N_{r}^{RF}, respectively. And both the transmitting end and the receiving end are single-stream communication. The received signal is:

$$\boldsymbol{Y} = \boldsymbol{W}^{\boldsymbol{H}}\boldsymbol{H}\boldsymbol{P}\boldsymbol{s} + \boldsymbol{n} \tag{1}$$

where $\boldsymbol{Y}$ is the receiving signal of the system, $\boldsymbol{W}$ is the hybrid combination matrix at the receiving end, $\boldsymbol{P}$ is the hybrid precoding matrix, $\boldsymbol{H}$ is the channel matrix, $\boldsymbol{s}$ is the pilot signal at the transmitter, $\boldsymbol{n}$ is the combined received Gaussian white noise.

The paper adopts the widely used Saleh-Valenzuela channel model

$$\boldsymbol{H} = \sqrt{\frac{N_t N_r}{L}} \sum_{l=1}^{L} \beta_l \mathbf{a}\left(\theta_{r,l}\right)\mathbf{a}^H\left(\theta_{t,l}\right) \tag{2}$$

where L is the effective propagation path ($L \ll \min(N_r, N_{\mathrm{t}})$), β_l is the complex gain of the l-th path, $\theta_{r,l}$ and $\theta_{t,l}$ are the corresponding arrival angle and transmit angle, respectively. $\mathbf{a}\left(\theta_{r,l}\right)$ and $\mathbf{a}\left(\theta_{t,l}\right)$ can be expressed as

$$\mathbf{a}(\theta_r) = \frac{1}{\sqrt{N_t}}\left[1, e^{j2\pi d \sin\theta_t/\lambda}, \ldots, e^{j2\pi(N-1)d \sin\theta_t/\lambda}\right]^T \tag{3}$$

$$\mathbf{a}(\theta_t) = \frac{1}{\sqrt{N_t}}\left[1, e^{j2\pi d \sin\theta_t/\lambda}, \ldots, e^{j2\pi(N-1)d \sin\theta_t/\lambda}\right]^T \tag{4}$$

where d = $\frac{\lambda}{2}$ is the distance between adjacent elements.

Therefore, the mmWave channel $\boldsymbol{H}$ can also be expressed as

$$\boldsymbol{H} = \boldsymbol{A}(\boldsymbol{\theta}_r)\boldsymbol{\beta}\boldsymbol{A}^{\mathrm{H}}(\boldsymbol{\theta}_t) \tag{5}$$

where $\boldsymbol{\beta} = \sqrt{\frac{N_t N_r}{L}} diag[\beta_1, \cdots, \beta_L]$.

Using $\mathbf{x}= \boldsymbol{Ps}$ to represent a pilot signal transmitted, the i-th element in vector $\boldsymbol{x}$ corresponds to the signal sent by the i-th transmitting antenna. The precoding matrix and the transmitted signal content $\mathrm{tr}(\boldsymbol{P}\boldsymbol{P}^{\mathrm{H}}) \leq \rho$ and $\mathrm{E}(\boldsymbol{s}\boldsymbol{s}^{\mathrm{H}}) = \boldsymbol{I}_N$, respectively. The received pilot signal can also be expressed as

$$\boldsymbol{Y} = \boldsymbol{U}^{\mathrm{H}}\boldsymbol{H}\boldsymbol{X} + \boldsymbol{N} \tag{6}$$

Due to the sparse nature of the channel, the sparse channel estimation problem can be transformed into

$$\min_{\hat{\boldsymbol{\beta}}, \hat{\boldsymbol{\theta}}_r, \hat{\boldsymbol{\theta}}_t} \left\| \hat{\boldsymbol{\beta}} \right\|_0, \text{ s.t.} \left\| \boldsymbol{Y} - \boldsymbol{U}^{\mathrm{H}}\hat{\boldsymbol{H}}\boldsymbol{X} \right\|_{\mathrm{F}} \leq \varepsilon \tag{7}$$

ε is a threshold set to control the estimation error.

3 Description of the Proposed Channel Estimation Algorithm

3.1 Proposed Optimization Alternative Formula

Generally speaking, the optimization of l_0-norm is difficult to solve, so in most researches, l_1-norm is often replaced by l_0-norm. However, in practice, due to the influence of random noise, a non-sparse solution is formed in the process of solving the l_1-norm. Therefore, this paper chooses a new regular term $l_{1/2}$-norm with stronger anti-noise ability to obtain a more sparse solution. The reason for choosing the $l_{1/2}$-norm is that the regular term we need is easier to solve than the l_0-norm, and at the same time obtain a sparser solution than the l_1-norm [7]. The sparse representation ability of the $l_q(0 < q < 1/2)$-norm is equivalent to that of the $l_{1/2}$-norm, and the $l_q(1/2 < q < 1)$-norm is weaker than the $l_{1/2}$-norm. Replacing the l_0-norm in the above formula with $l_{1/2}$-norm to get

$$\min_{\boldsymbol{\beta}, \boldsymbol{\theta}_r, \boldsymbol{\theta}_t} F(\boldsymbol{\beta}) = \|\boldsymbol{\beta}\|_{1/2}, \text{ s.t.} \left\| \boldsymbol{Y} - \boldsymbol{U}^{\mathrm{H}}\hat{\boldsymbol{H}}\boldsymbol{X} \right\|_{\mathrm{F}} \leq \varepsilon \tag{8}$$

γ is introduced to control the error between sparsity and data fitting. The problem (8) can be refactored into the following form

$$\min_{\boldsymbol{\beta}, \boldsymbol{\theta}_r, \boldsymbol{\theta}_t} G(\boldsymbol{\beta}, \boldsymbol{\theta}_r, \boldsymbol{\theta}_t) = \|\, \boldsymbol{\beta}\|_{1/2} + \gamma \left\| \boldsymbol{Y} - \boldsymbol{U}^{\mathrm{H}}\hat{\boldsymbol{H}}\boldsymbol{X} \right\|_F^2 \tag{9}$$

The $l_q(0 < q < 1)$-norm has non-convex characteristic, and its solution can be transformed into an iterative convex optimization process, which is a form of equivalent replacement. The specific expression is

$$\underset{\boldsymbol{\beta},\boldsymbol{\theta}_r,\boldsymbol{\theta}_t}{min} S^{(t)}(\boldsymbol{\beta},\boldsymbol{\theta}_r,\boldsymbol{\theta}_t) \triangleq \sum_{i=1}^{L}\left(\left(\boldsymbol{\beta}_i^{(t)}\right)^2+\delta\right)^{-3/4}\boldsymbol{\beta}_i^2+\gamma\left\|\boldsymbol{Y}-\boldsymbol{U}^{\mathrm{H}}\hat{\boldsymbol{H}}\boldsymbol{X}\right\|_F^2 \tag{10}$$

Based on the above statements, this paper constructs an iterative proxy function for formula (10). Then the solution $G(\boldsymbol{\beta},\boldsymbol{\theta}_r,\boldsymbol{\theta}_t)$ can be converted into an optimization problem of substitution function [6].

$$\min_{\boldsymbol{\beta},\boldsymbol{\theta}_r,\boldsymbol{\theta}_t} S^{(t)}(\boldsymbol{\beta},\boldsymbol{\theta}_r,\boldsymbol{\theta}_t) \triangleq \boldsymbol{\beta}^H\boldsymbol{D}^{(t)}\boldsymbol{\beta}+\gamma\left\|\boldsymbol{Y}-\boldsymbol{U}^{\mathrm{H}}\hat{\boldsymbol{H}}\boldsymbol{X}\right\|_F^2 \tag{11}$$

where

$$\boldsymbol{D}^{(t)} \triangleq diag\left[\frac{1}{\left(\left(\hat{\boldsymbol{\beta}}_{i1}^{(t)}\right)^2+\delta\right)^{3/4}}\frac{1}{\left(\left(\hat{\boldsymbol{\beta}}_{i2}^{(t)}\right)^2+\delta\right)^{3/4}}\cdots\frac{1}{\left(\left(\hat{\boldsymbol{\beta}}_{iL}^{(t)}\right)^2+\delta\right)^{3/4}}\right] \tag{12}$$

In (10), we will encounter a situation. This situation is when $\boldsymbol{\beta}_i^{(t)} = 0$, if δ is not introduced, (10) will be undefined. Therefore, in the alternative optimization process, this article not only needs to introduce δ. In order to obtain better estimation performance, the parameters will gradually decrease in the iterative process instead of a fixed value [8].

In the t-th iteration, $\hat{\boldsymbol{\beta}}^{(t+1)}$, $\hat{\boldsymbol{\theta}}_r^{(t+1)}$, and $\hat{\boldsymbol{\theta}}_t^{(t+1)}$ will be found so that $S^{(t)}(\boldsymbol{\beta},\boldsymbol{\theta}_r,\boldsymbol{\theta}_t)$ satisfies the following inequality

$$S^{(t)}(\hat{\boldsymbol{\beta}}^{(t+1)},\hat{\boldsymbol{\theta}}_r^{(t+1)},\hat{\boldsymbol{\theta}}_t^{(t+1)}) \le S^{(t)}(\hat{\boldsymbol{\beta}}^{(t)},\hat{\boldsymbol{\theta}}_r^{(t)},\hat{\boldsymbol{\theta}}_t^{(t)}) \tag{13}$$

Combining (9), (10) and (11), we have

$$\begin{aligned} &G\left(\hat{\boldsymbol{\beta}}^{(t+1)},\hat{\boldsymbol{\theta}}_r^{(t+1)},\hat{\boldsymbol{\theta}}_t^{(t+1)}\right)-S^{(t)}\left(\hat{\boldsymbol{\beta}}^{(t+1)},\hat{\boldsymbol{\theta}}_r^{(t+1)},\hat{\boldsymbol{\theta}}_t^{(t+1)}\right)\\ &=F\left(\hat{\boldsymbol{\beta}}^{(t+1)}\right)-\sum_{l=1}^{L}\frac{\left|\hat{\boldsymbol{\beta}}^{(t+1)}\right|^2}{\left(\left|\hat{\boldsymbol{\beta}}^{(t+1)}\right|^2+\delta\right)^{3/4}}\end{aligned}$$

$$\le F\left(\hat{\boldsymbol{\beta}}^{(t)}\right) - \sum_{l=1}^{L} \frac{\left|\hat{\boldsymbol{\beta}}^{(t)}\right|^2}{\left(\left|\hat{\boldsymbol{\beta}}^{(t)}\right|^2 + \delta\right)^{3/4}}$$

$$= G\left(\hat{\boldsymbol{\beta}}^{(t)}, \hat{\boldsymbol{\theta}}_r^{(t)}, \hat{\boldsymbol{\theta}}_t^{(t)}\right) - S^{(t)}\left(\hat{\boldsymbol{\beta}}^{(t)}, \hat{\boldsymbol{\theta}}_r^{(t)}, \hat{\boldsymbol{\theta}}_t^{(t)}\right) \tag{14}$$

It is worth noting that when $\boldsymbol{\beta} = \hat{\boldsymbol{\beta}}^{(t)}$, $G(\boldsymbol{\beta}, \boldsymbol{\theta}_r, \boldsymbol{\theta}_t) - S^(\mathrm{t})(\boldsymbol{\beta}, \boldsymbol{\theta}_r, \boldsymbol{\theta}_t)$ gets the maximum. And we can get

$$\begin{aligned}
&G(\hat{\boldsymbol{\beta}}^{(t+1)}, \hat{\boldsymbol{\theta}}_r^{(t+1)}, \hat{\boldsymbol{\theta}}_t^{(t+1)}) \\
&= G(\hat{\boldsymbol{\beta}}^{(t+1)}, \hat{\boldsymbol{\theta}}_r^{(t+1)}, \hat{\boldsymbol{\theta}}_t^{(t+1)}) - S^{(t)}(\hat{\boldsymbol{\beta}}^{(t+1)}, \hat{\boldsymbol{\theta}}_r^{(t+1)}, \hat{\boldsymbol{\theta}}_t^{(t+1)}) \\
&\quad + S^{(t)}(\hat{\boldsymbol{\beta}}^{(t+1)}, \hat{\boldsymbol{\theta}}_r^{(t+1)}, \hat{\boldsymbol{\theta}}_t^{(t+1)}) \\
&\le G(\hat{\boldsymbol{\beta}}^{(t)}, \hat{\boldsymbol{\theta}}_r^{(t)}, \hat{\boldsymbol{\theta}}_t^{(t)}) - \left[S^{(t)}(\hat{\boldsymbol{\beta}}^{(t)}, \hat{\boldsymbol{\theta}}_r^{(t)}, \hat{\boldsymbol{\theta}}_t^{(t)}) - S^{(t)}(\hat{\boldsymbol{\beta}}^{(t+1)}, \hat{\boldsymbol{\theta}}_r^{(t+1)}, \hat{\boldsymbol{\theta}}_t^{(t+1)})\right] \\
&\le G(\hat{\boldsymbol{\beta}}^{(t)}, \hat{\boldsymbol{\theta}}_r^{(t)}, \hat{\boldsymbol{\theta}}_t^{(t)})
\end{aligned} \tag{15}$$

To simplify $S^{(t)}(\boldsymbol{\beta}, \boldsymbol{\theta}_r, \boldsymbol{\theta}_t)$, this algorithm constructs two functions. One is to use $\boldsymbol{\theta}_r$ and $\boldsymbol{\theta}_t$ to represent the correlation function of $\boldsymbol{\beta}$, and the other is to use $\boldsymbol{\theta}_r$ and $\boldsymbol{\theta}_t$ to represent the function of S. The specific expression is as follows

$$\boldsymbol{\beta}_{opt}^{(t)} \triangleq arg \min_{\boldsymbol{\beta}} S^{(t)}(\boldsymbol{\beta}, \boldsymbol{\theta}_r, \boldsymbol{\theta}_t) = \left(\gamma^{-1}\boldsymbol{D}^{(t)} + \boldsymbol{K}^H\boldsymbol{K}\right)^{-1}\left(\boldsymbol{K}^H\boldsymbol{Y}\right) \tag{16}$$

where

$$K = \boldsymbol{U}^H \boldsymbol{A}(\boldsymbol{\theta}_r) diag\left(\boldsymbol{A}^H(\boldsymbol{\theta}_t)\boldsymbol{X}\right) \tag{17}$$

Finally, substituting (16) into (11), it converts $S^{(t)}(\boldsymbol{\beta}, \boldsymbol{\theta}_r, \boldsymbol{\theta}_t)$ into a function only related to the angle parameter.

$$\begin{aligned}
S_{opt}^{(t)}(\boldsymbol{\theta}_r, \boldsymbol{\theta}_t) &\triangleq \min_{\boldsymbol{\beta}} S^{(t)}(\boldsymbol{\beta}, \boldsymbol{\theta}_r, \boldsymbol{\theta}_t) = -\left(\boldsymbol{K}^H\boldsymbol{Y}\right)^H\left(\gamma^{-1}\boldsymbol{D}^{(t)}\boldsymbol{K}^H\boldsymbol{K}\right)^{-1} \\
&\quad + \left(\boldsymbol{K}^H\boldsymbol{Y}\right) + \boldsymbol{Y}^H\boldsymbol{Y}
\end{aligned} \tag{18}$$

After that, in (5), we only need to estimate $\boldsymbol{\theta}_r$ and $\boldsymbol{\theta}_t$.

3.2 Channel Estimation Based on IR

In order to solve the problem of angle parameter estimation the IR-based channel estimation method is used in this paper.

γ is used to adjust the weight between $\boldsymbol{\beta}^H \boldsymbol{D}^{(t)} \boldsymbol{\beta}$ and $\|\boldsymbol{Y} - \boldsymbol{K}\boldsymbol{\beta}\|_F^2$. γ will be updated in the following ways

$$\gamma = \min(d/r^{(t)}, \gamma_{\max}) \tag{19}$$

where $\gamma_{\max}$ is used to ensure the good operation of the algorithm. $r^{(t)}$ is the residual square of the previous iteration.

$$r^{(t)} = \left\| \boldsymbol{Y} - \boldsymbol{U}^H \boldsymbol{A}(\widehat{\boldsymbol{\theta}}_r^{(t)}) \widehat{\boldsymbol{\beta}}^{(t)} \boldsymbol{A}^H (\widehat{\boldsymbol{\theta}}_t^{(t)}) \boldsymbol{X} \right\|_F^2 \tag{20}$$

The algorithm uses gradient descent method to estimate the angle parameters. The method is expressed as follows

$$\begin{aligned} \widehat{\boldsymbol{\theta}}_r^{(t+1)} &= \widehat{\boldsymbol{\theta}}_r^{(t)} - \varsigma \cdot \nabla_{\boldsymbol{\theta}_r} S_{opt}^{(t)} (\widehat{\boldsymbol{\theta}}_r^{(t)}, \widehat{\boldsymbol{\theta}}_t^{(t)}) \\ \widehat{\boldsymbol{\theta}}_t^{(t+1)} &= \widehat{\theta}_t^{(t)} - \varsigma \cdot \nabla_{\boldsymbol{\theta}_t} S_{opt}^{(t)} (\widehat{\boldsymbol{\theta}}_r^{(t)}, \widehat{\boldsymbol{\theta}}_t^{(t)}) \end{aligned} \tag{21}$$

where ∇ is the gradient operator, ς is the step size.

In this algorithm, a SVD-based scheme is used to initialize the angle parameters. The received signal $\boldsymbol{Y}$ is simplified by SVD. We have $\boldsymbol{Y} = \boldsymbol{W}\Sigma\boldsymbol{V}^H$, Σ is a diagonal matrix. The angle parameter initialization formula is expressed as

$$\begin{aligned} \widehat{\boldsymbol{\theta}}_r^{(0)} &= \operatorname{argmin} \boldsymbol{W}^H \boldsymbol{U}^H \boldsymbol{A}(\boldsymbol{\theta}_r) \\ \widehat{\boldsymbol{\theta}}_t^{(0)} &= \operatorname{argmin} \boldsymbol{V}^H \boldsymbol{X}^H \boldsymbol{A}(\boldsymbol{\theta}_t) \end{aligned} \tag{22}$$

The pre-processing method based on SVD can debase the complexity and at the same time find the angular domain grid closest to the real AoA/AoD.

Algorithm 1. The specific Flow of the Algorithm

Input	The receive signal $\boldsymbol{Y}$; Initialize the angle parameter $\hat{\boldsymbol{\theta}}_{\mathrm{r}}^{(0)}$ and $\hat{\boldsymbol{\theta}}_{\mathbf{t}}^{(0)}$; Delete threshold β_{th}; Fault tolerance threshold $\varepsilon_{\mathrm{th}}$
Step 1	Initialize $\hat{\boldsymbol{\beta}}^{(0)} = \boldsymbol{\beta}_{\boldsymbol{opt}}(\hat{\boldsymbol{\theta}}_{\mathbf{r}}^{(0)}, \hat{\boldsymbol{\theta}}_{\mathbf{t}}^{(0)})$ according to (16)
Step 2	Update γ by (20)
Step 3	Calculated $\boldsymbol{S}_{\mathrm{opt}}^{(}\mathrm{t})(\boldsymbol{\theta}_{\mathbf{r}}, \boldsymbol{\theta}_{\mathbf{t}})$ by (18)
Step 4	Estimate the new $\hat{\boldsymbol{\theta}}_{\mathbf{r}}^{(\mathrm{t}+1)}$ and $\hat{\boldsymbol{\theta}}_{\mathbf{t}}^{(\mathrm{t}+1)}$ by (22)

(continued)

(continued)

Input	The receive signal $\boldsymbol{Y}$; Initialize the angle parameter $\hat{\boldsymbol{\theta}}_{\mathrm{r}}^{(0)}$ and $\hat{\boldsymbol{\theta}}_{\mathbf{t}}^{(0)}$; Delete threshold β_{th}; Fault tolerance threshold $\varepsilon_{\mathrm{th}}$
Step 5	Estimate $\hat{\boldsymbol{\beta}}^{(\mathrm{t}+1)}$ by (16); If $\hat{\boldsymbol{\beta}}_{l}^{(\mathrm{t}+1)} < \beta_{\mathrm{th}}$, then trim the path
Step 6	Until $L^{(\mathrm{t})} = L^{(\mathrm{t}+1)}$ and $\left\| \hat{\boldsymbol{\beta}}^{(\mathrm{t}+1)} - \hat{\boldsymbol{\beta}}^{(\mathrm{t})} \right\|_{2} < \varepsilon_{\mathrm{th}}$, the iteration ends

4 Simulation Results

The properties of the proposed algorithm is verified through some simulation comparison results in this section.

The simulation parameter is set to $N_{\mathrm{t}} = N_{\mathrm{r}} = 64$. We use four algorithms for comparison, including LS-based channel estimation, OMP-based channel estimation, ADMM-based channel estimation [9], and Cramer-Rao bound (CRB).

Figure 1a shows the NMSE for channel estimation of various algorithms under different SNRs. The accuracy of each algorithm increases as the SNR increases. The performance of the LS-based algorithm has the worst estimation accuracy and almost no change, indicating that the traditional LS is not suitable for mmWave massive MIMO channel estimation. This is mainly due to the easy attenuation characteristics of mmWave, and its estimated environment is often low SNR. From the overall effect, the proposed algorithm is closer to CRB.

The effect of path numbers on the NMSE of the four algorithms is shown in Fig. 1b. Figure 1b shows that with the number of paths increases, the estimation accuracy of the three algorithms show a downward trend. Under the same number of

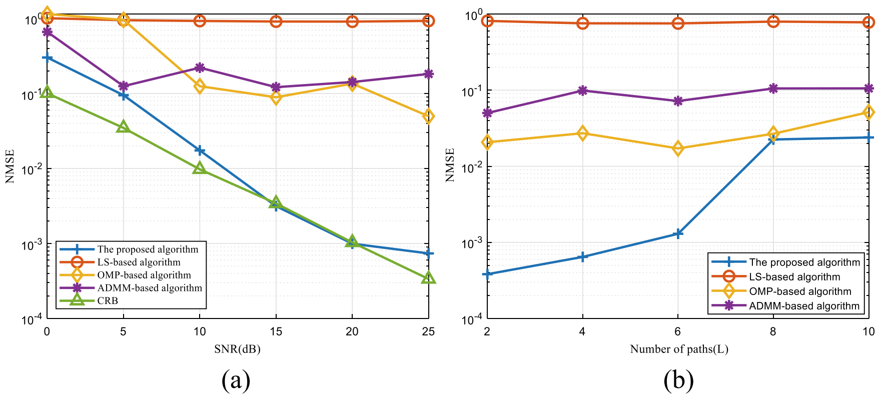

Fig. 1 **a** NMSE versus SNR. **b** NMSE versus L

paths, the channel estimation performance of the proposed algorithm is better than the other algorithms.

In summary, the traditional channel estimation method is not suitable for mm-Wave massive MIMO system to a certain extent. The proposed algorithm based on CS becomes a better choice.

5 Conclusion

In short, a channel estimation method based on $l_{1/2}$-SVD is proposed. The basic idea of the algorithm is to transform the channel estimation into the recovery of sparse signals. The iterative replacement function based on $l_{1/2}$ is constructed first, and then preprocessed by SVD, which reduces the computational complexity. Finally, the objective function is optimized by the gradient descent method to obtain the optimal solution of the angle parameter. After simulation analysis, it can be gained that the proposed algorithm has certain advantages and provides guidance for subsequent channel estimation algorithm research.

Acknowledgements This work was supported by the National Natural Science Foundation of China (No. 61861015 and 61961013), Key Research and Development Program of Hainan Province (No. ZDYF2019011), National Key Research and Development Program of China (No. 2019CXTD400), Young Elite Scientists Sponsorship Program by CAST (No. 2018QNRC001), and the Scientific Research Setup Fund of Hainan University (No. KYQD(ZR) 1731).

References

1. Cong, J., Wang, X., Huang, M., Wan, L.: Robust DOA estimation method for MIMO radar via deep neural networks. IEEE Sens. J. **21**(6), 7498–7507 (2020)
2. Wang, X., Yang, L.T., Meng, D., Dong, M., Ota, K., Wang, H.: Multi-UAV cooperative localization for marine targets based on weighted subspace fitting in SAGIN environment. IEEE Internet Things J. (2021)
3. Wang, X., Wan, L., Huang, M., Shen, C., Han, Z., Zhu, T.: Low-complexity channel estimation for circular and noncircular signals in virtual MIMO vehicle communication systems. IEEE Trans. Veh. Technol. **69**, 3916–3928 (2021)
4. Shao, J., Wang, X., Lan, X., et al.: GAMP-SBL-based channel estimation for millimeter-wave MIMO systems. EURASIP J. Adv. Signal Process. **1**, 1–22 (2021)
5. Hu, C., Dai, L., Gao, Z., Fang, J.: Super-resolution channel estimation for MmWave massive MIMO with hybrid precoding. IEEE Trans. Veh. Technol. **67**, 8954–8958 (2018)
6. Zhang, Z., Liang, Y., Gui, G.: -Regularization based sparse channel estimation for MmWave massive MIMO systems. In: IEEE 23rd International Conference on Digital Signal Processing (2018)
7. Zhang, Z., Liang, Y., Shi, W., Yuan, L., Gui, G.: Regularization based super-resolution sparse channel estimation for MmWave massive MIMO systems. IEEE Access **7**, 75837–75844 (2019)
8. Wang, X., Huang, M., Wan, L.: Joint 2D-DOD and 2D-DOA estimation for coprime EMVS–MIMO radar. In: Circuits, Systems, and Signal Processing (2021)

9. Vlachos, E., Alexandropoulos, G.C., Thompson, J.: Massive MIMO channel estimation for millimeter wave systems via matrix completion. IEEE Signal Process. Lett. **25**(11), 1675–1679 (2018)